JMEPEG (2004) 13:200-207
DOI: 10.1361/10599490418415

1059-9495/$19.00

Study on High Strain Rate Superplasticity of A 6061Al Alloy Composite Reinforced With 30 Vol.% AlN Particulate

Lihong Han, Jitai Niu, Henry Hu, and Derek O. Northwood

(Submitted 20 November 2003; in revised form 5 January 2004)

An investigation on the superplastic behavior of 30 vol.% AlNp/6061Al composite prepared by powder metallurgy (PM) techniques was carried out. Superplastic tensile tests of the composite were performed at strain rates ranging from 10° to 10^{-3} s^{-1} and at temperatures from 823 to 893 K. A fine-grained structure prior to superplastic testing was obtained by hot rolling after extrusion. The highest total elongation to failure of 438% was achieved at a temperature of 863 K and at an initial strain rate of 1.67×10^{-1} s^{-1} and the highest value of the strain rate sensitivity index (m) was 0.42 for the composite. Differential thermal analysis (DTA) was used to investigate the possibility of any partial melting in the vicinity of optimum superplastic temperatures. The formation of a liquid phase is attributed to the melting of the Al-Si eutectic phase at the surface of the AlN particulates at elevated temperatures, as determined by electron probe microanalysis (EPMA). The influence of the microstructure and the fracture behavior on the superplastic behavior of the composite was studied by transmission electronic microscopy (TEM) and scanning electron microscopy (SEM). A large number of matrix filaments were present at the fracture surfaces of the specimens when superplastic deformation of the composite was performed under the optimum superplastic test conditions. The presence of dislocations and fine recrystallized grains in the test specimens suggested that they play an important role in the high-strain-rate superplasticity for this composite.

Keywords Al matrix composite, AlN particulate, superplasticity

1. Introduction

Metal matrix composites (MMCs) reinforced with discontinuous reinforcements such as particles and whiskers have been successfully prepared by power metallurgy methods in recent years. Due to their high specific strength and modulus of elasticity, they have great potential for application in many fields of structural engineering. It has been demonstrated that some discontinuously reinforced aluminum (Al) matrix composites exhibit high strain rate superplasticity (HSRS) with total elongations of 250-600% at strain rates ranging from 0.1 to 10 s^{-1}.[1-17] Scientific understanding of the HSRS behavior is of great significance not only for superplasticity itself but also for the processing of metal-matrix composites. This is because one of the major drawbacks of conventional superplasticity is that it occurs at low strain rates, typically from 10^{-3} to 10^{-4} s^{-1}. More importantly, HSRS of composites could potentially be used to develop energy-efficient and cost-effective near-net shape manufacturing technologies for various automotive and aerospace applications.

The main deformation mechanisms of HSRS composites are grain boundary sliding and interfacial sliding at a liquid phase when HSRS occurs at temperatures above, or slightly below, the solidus temperature of the composite. However, it is not yet clear how some superplastic factors, such as a liquid phase at the interface, dislocation behavior in the matrix, and the recrystallization process, are associated with the accommodation mechanisms for HSRS deformation. This study presents experimental evidence to show that high elongations (over 300%) to failure can be achieved at relatively high strain rates in an AlNp/6061Al composite prepared by a powder metallurgyPM method. The effect of the liquid phase at the interface and dislocations concentrating near the interfaces (grain boundary-grain boundary and matrix-reinforcement) on superplasticity of the composite is discussed. The activation energy for superplastic deformation of the composite is compared with those for unreinforced Al and other Al MMCs.

Lihong Han, Henry Hu, and **Derek O. Northwood,** Department of Mechanical, Automotive and Materials Engineering, University of Windsor, Windsor, Ontario, N9B 3P4, Canada; and **Jitai Niu,** The National Key Laboratory of Advanced Welding Production Technology, Harbin Institute of Technology; Harbin, Heilongjiang Province, 150001, People's Republic of China. Contact e-mail: dnorthwo@uwindsor.ca.

2. Experimental Details

2.1 Materials and Specimen Preparation

The 30 vol.% AlN particles with an average size of 1.78 μm and the atomized powders of 6061Al alloy were mechanically stirred and ultrasonically mixed in an alcohol solvent and then dried in air. The distribution of AlN particulate sizes is shown in Fig. 1. The chemical composition of 6061Al alloy is shown in Table 1. The mixed powders were first cold-pressed in an Al can and degassed in vacuum. They were then hot-pressed at a pressure of 200 MPa for 20 min, and then forged at 773 K in air at a constant pressure of 495 MPa for 20 min. The consolidated billets were extruded at a temperature of 773 K with an extrusion ratio of 44:1. After being heated in the desired tem-

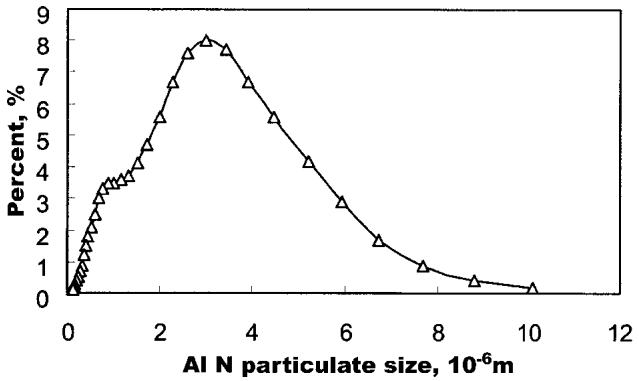

Fig. 1 The distribution of AlN particulate sizes with an average size of 1.78μm

Table 1 Chemical Composition of 6061Al Alloy Used as Matrix in the Fabrication of the Composite (mass%)

Alloy	Fe	Cu	Mn	Mg	Cr	Si	Al
6061Al	0.24	0.26	0.06	0.83	0.07	0.82	Balance

perature range, the extruded billets were hot rolled at 673, 723, and 813 K, respectively. The strain for each rolling pass was less than 0.1 and the reheating-holding time between each rolling pass was roughly 5 min. The final thickness of the hot-rolled composite was around 0.8 mm. Tensile specimens with a cross section of 4 × 0.8 mm and a gauge length of 5 mm were machined from the hot-rolled sheet in a direction which was parallel to the extrusion and hot-rolling direction.

2.2 Tensile Testing

Tensile testing was conducted in a three-zone split furnace with three independent proportional temperature controllers. Prior to each test, the specimens were held in the furnace at the test temperature for 10 min to equilibrate the specimen temperature. All the tests were conducted in air. The initial strain rates produced by different constant crosshead velocities ranged from 10° to 10^{-3} s^{-1}.

2.3 Microstructural Analysis

The shape, size, and distribution of the reinforcement in the matrix and the morphology of the surface of the fractured specimens were observed using a Hitachi S-570 (Tokyo, Japan) scanning electron microscope (SEM). The microstructure of the composite, including the characteristics of grains and dislocations, and the interface structure between the reinforcement and the matrix, were investigated using a Hitachi H800 transmission electron microscope (TEM) operating at 100-120 kV. Specimens for TEM were prepared using a Gatan-600 (Pleasanton, CA) ion beam-milling machine at 5 kV and 1 mA. The line distribution of the elemental concentration at the interface between the reinforcement and the matrix were determined using electron probe microanalysis (EPMA). A relatively large AlN particulate was intentionally used to facilitate the analysis of element segregation at the interface. To assess the solidus and liquidus temperatures of the composite, thermal analysis was performed using a Rigaku Denki TAS100-DTA (Tokyo, Japan). Differential thermal analysis (DTA) samples were analyzed from room temperature to 973K at a heating rate of 10K/min.

3. Results and Discussion

3.1 Microstructure

The SEM micrographs in Fig. 2(a) and (b) show the distribution of the AlN particles in the 30 vol.% AlNp/6061Al composite. It is evident that there is a more uniform distribution of AlN particles throughout the matrix for the as-rolled composite (Fig. 2b) compared with the as-extruded composite (Fig. 2a), in which there is some localized poor and rich areas of AlN particles. Therefore, to make the distribution of AlN particles in the composite more uniform, hot rolling was used to improve the properties of the composites after they were extruded. This pretreatment process may not only eliminate some micro-defects, such as microcracks and porosity in the composite, but may also contribute to the formation of dislocations and fine recrystallized grains in the composite. The TEM micrograph in Fig. 3 shows a "clear" interface between the matrix and the reinforcement with no reaction products or other micro-defects.

3.2 Superplastic Behavior

3.2.1 Effect of Rolling Temperature. Figure 4 shows the relationship between the flow stress and the strain rate at a test temperature of 863 K as a function of rolling temperature. Flow stress is the instantaneous yield stress or true stress of a metal defined as a function of material-related factors (composition, microstructure, grain size, prior strain history) and process-related factors (temperature of deformation, degree of deformation strain rate of deformation or strain rate). It can be seen that, in general, the flow stress increases with increasing rolling temperature from 673-723 K to 813 K at all strain rates. For all three rolling temperatures, an increase in strain rate results in a higher flow stress for the superplastic deformation of the composite. Superplastic deformation of the composite rolled at 813 K gives rise to the highest flow stress (8.3 MPa) at a strain rate of 1.0 s^{-1} for the composites rolled at all three temperatures. The lowest flow stress (roughly 0.5 MPa) at a strain rate of 10^{-3} s^{-1} is observed for the superplastic deformation of the composite rolled at 673 K.

The total elongation to failure of the composites hot-rolled at the three temperatures from 673-723 K to 813 K is shown in Fig. 5. Prior to superplastic deformation, rolling is often used as a pre-process step to not only minimize internal defects such as porosity, densify the material, and refine the grain structure, but also to homogenize the distribution of reinforcements in the composite.[2] Rolling parameters such as ingot temperature can significantly influence the superplastic behavior of a material. It is worthwhile mentioning that, corresponding to each rolling temperature, there is an optimum strain rate range where relatively high total elongations to failure are achieved. A rolling temperature of 813 K produces the highest total elongation to failure for the composites tested. Compared with a rolling tem-

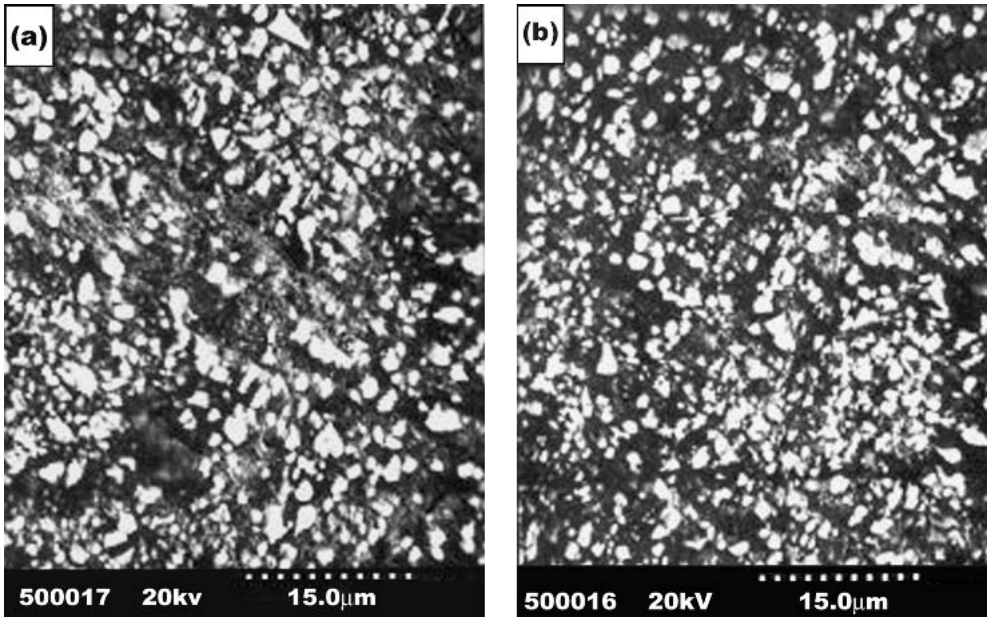

Fig. 2 The distribution of AlN particulate reinforcement in the matrix of a 6061Al alloy: **(a)** as-extruded and **(b)** as-rolled after extrusion

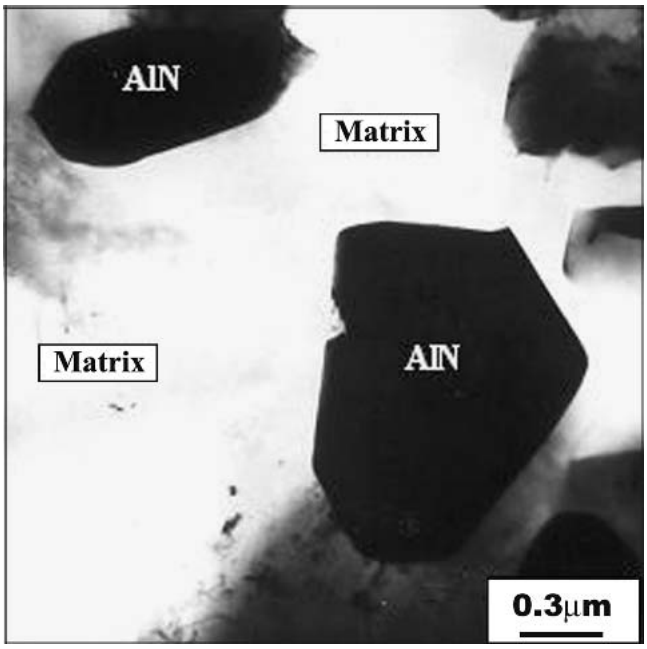

Fig. 3 TEM image of the interface between the matrix and the reinforcement

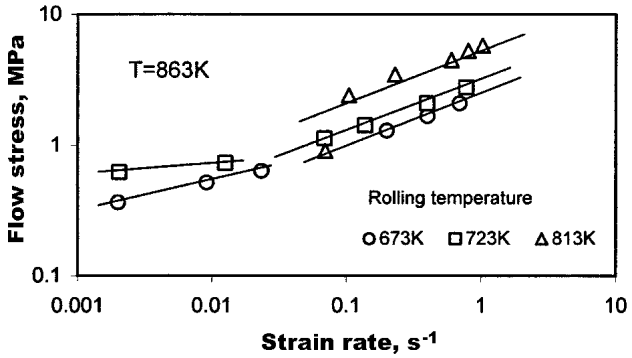

Fig. 4 Relationship between flow stress and strain rate at three different hot-rolling temperatures at a superplastic test temperature of 863 K

perature of 723 K, the composites hot-rolled at 813 and 673 K exhibit higher total elongations to failure, more than 300% at a strain rate of 1.67×10^{-1} s^{-1}. The effect of the rolling temperature on the superplastic behavior may be attributed to an increase in dislocation density and microcrack formation due to the fracture of AlN particles inside the composite during rolling. A further investigation in the influence of rolling temperatures is needed for a better understanding of this behavior.

3.2.2 Effect of Testing Temperature. The relationship between the total elongation-to-failure and the initial strain rate at different test temperatures is shown in Fig. 6. As can be seen, a relatively low elongation (100% at 823 K and 240% at 863 K) was achieved at low strain rates, slightly higher than1.0×10^{-3} s^{-1}. A maximum elongation of 438% was obtained at a strain rate of 1.67×10^{-1} s^{-1} at a testing temperature close to 863 K. Above this strain rate, and within the range of test temperatures (823-893 K), the total elongation to failure of the composite tends to decrease. It can also be seen that the elongation peak for the composite moves from a low value of strain rate to a high value of strain rate as test temperature increases. To interpret the observed superplasticity behavior the phase transformation temperatures of the composite need to be determined. A typical DTA curve for the composite is shown in Fig. 7. The DTA results show that the as-rolled composite with 30 vol.% of reinforcement has a solidus temperature of 851 K and a full melting temperature of 904 K. The optimum superplastic temperature at which a maximum elongation becomes achievable is often close to, or slightly above, the solidus temperature

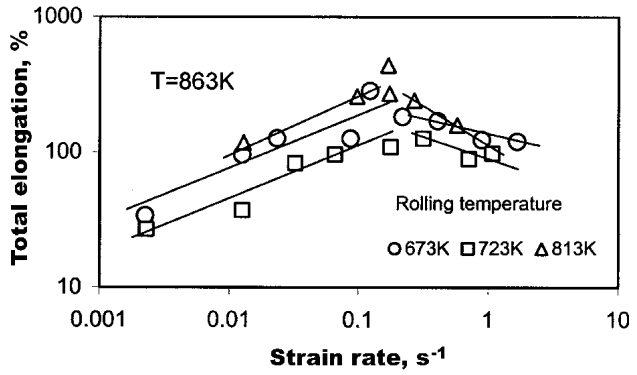

Fig. 5 Relationship between total elongation to failure and strain rate at three different hot-rolling temperatures at a superplastic test temperature of 863 K

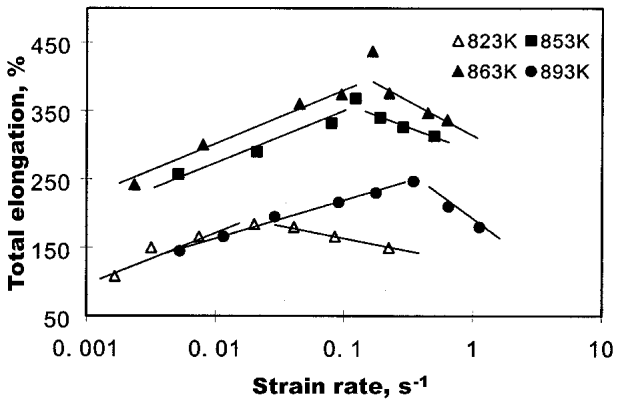

Fig. 6 Relationships between total elongation and initial strain rate at different test temperatures for the AlNp/6061Al composite

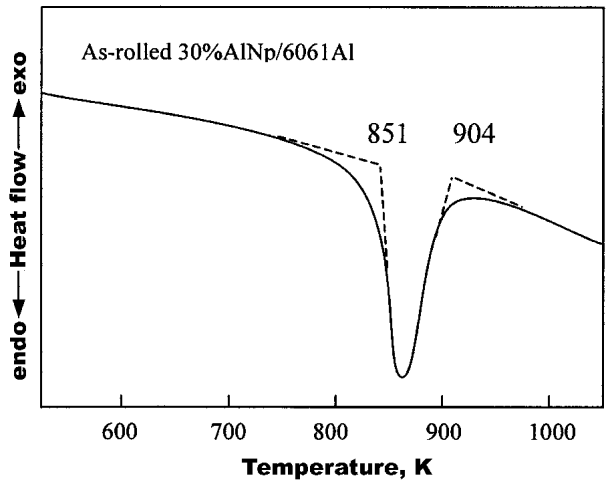

Fig. 7 DTA result of 30% AlNp/6061Al composite

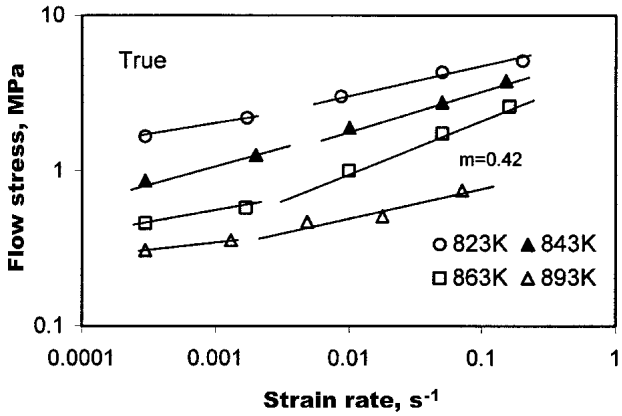

Fig. 8 Relationship between flow stress and initial strain rate for AlNp/6061Al composites

of the material.[6,9] This indicates that the optimum superplasticity of the composite should take place around its solidus temperature of 851 K. A 438% elongation is obtained at a strain rate of 1.67×10^{-1} s^{-1} and a temperature of 863 K, which is slightly higher than the solidus temperature of the composite. This result shows that the composite has exhibited the excellent high-strain-rate superplasticity with the optimum test temperatures and strain rates. However, at a temperature of 893 K, which is 42 K higher than the solidus temperature, a lower total elongation of 150% was measured. This may result from the presence of relatively large amounts of liquid phase at the grain boundaries, and at the interface between matrix and reinforcement, which significantly reduces the elongation of the composite.

Figure 8 shows the relationship between the flow stress and the strain rate for different test temperatures ranging from 823 to 893 K. The results show that the flow stress at all test temperatures increases with increasing strain rate. The strain rate sensitivity m is a characteristic parameter of superplastic materials. Materials that have high m value usually exhibit superplasticity. At the same time, a large elongation can be obtained. The strain rate sensitivity m at a constant strain ε, and temperature T, can be determined by the following equation:

$$m = \left[\frac{\partial(\ln \sigma)}{\partial(\ln \dot{\varepsilon})}\right] T,\varepsilon = 0.2 \qquad \text{(Eq 1)}$$

where σ is a flow stress and $\dot{\varepsilon}$ is a true strain rate at the true strain of 0.2.[18] For the present composite, the strain rate sensitivity is relatively low in the low strain rate regimen below 10^{-2} s^{-1} over a temperature range of 823-893 K. In the high strain rate range from 10^{-2} to 10^{-1} s^{-1}, a relatively high m value of 0.38-0.42 was observed in the temperature range of 853-873 K. The maximum value of m is obtained under the optimum superplastic conditions, which means the composite exhibits high-strain-rate superplastic behavior. At the same time, the relatively high values of m suggest that the large elongations for the composite result from the suppression of necking during superplastic deformation. However, if superplastic deformation temperatures are too low (less than 853 K) or too high (more than 873 K), even if strain rates are high, the composite did not exhibit high-strain-rate superplastic behavior and the m value is very low. The characteristics of the flow stress-strain rate curve for the composite, which exhibit high-strain-rate superplasticity, are similar to those of a conventional superplastic curve.

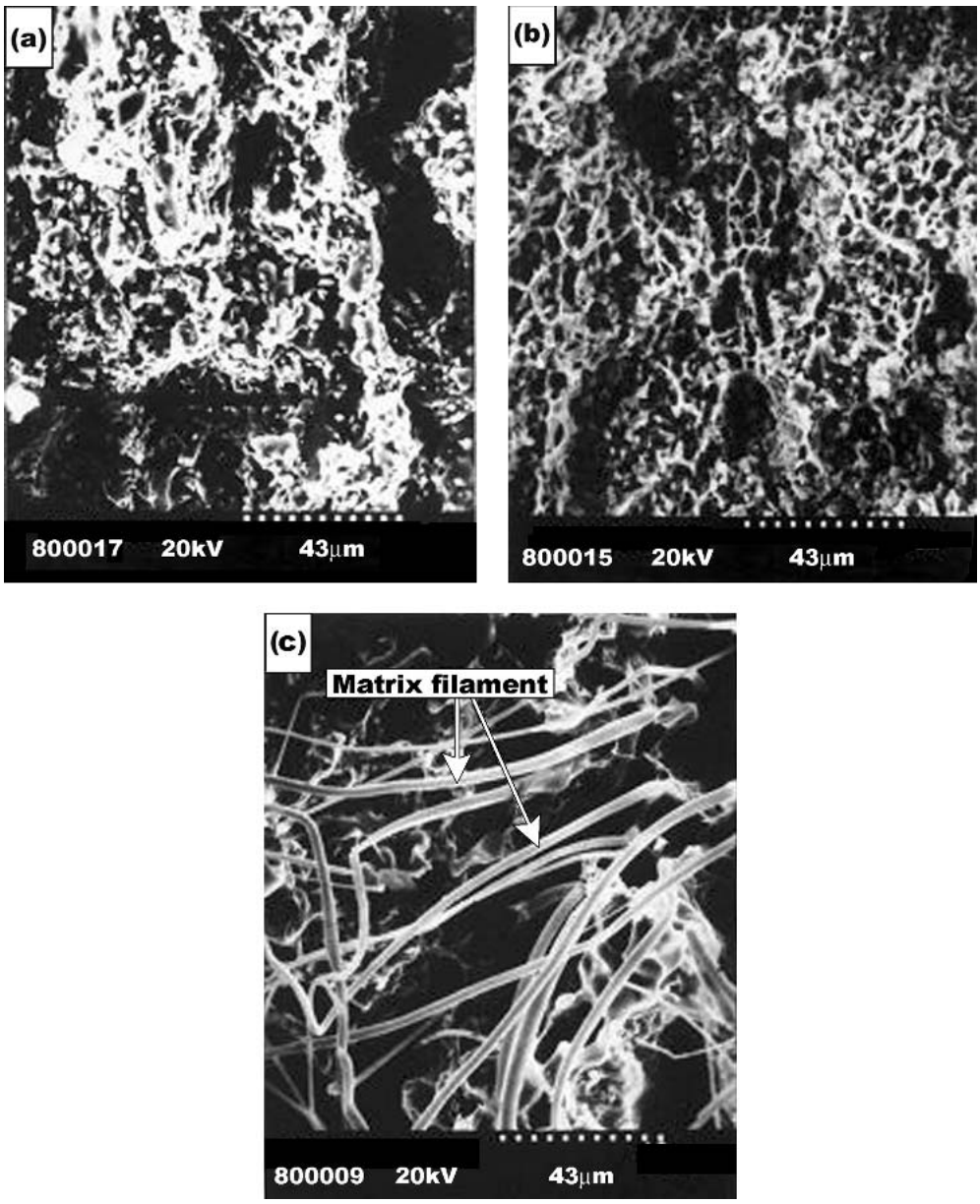

Fig. 9 SEM of fracture surface of the composite tested at **(a)** 823 K, **(b)** 843 K, and **(c)** 863 K

3.3 Fracture Behavior

Examination of the fracture surfaces of the test specimens using SEM showed that the fracture behavior of the 30 vol.% AlNp/6061Al composite is influenced by test temperature. Figures 9(a)-(c) show the fracture surfaces of the composites tested at 823, 843, and 863 K at an initial strain rate of 1.67×10^{-1} s^{-1}. The smooth and scalelike fracture surface suggests low superplasticity for the composites deformed at 823 and 843 K. However, as the test temperature increases, the superplasticity of the composite gradually improves. Deep dimple patterns and the long threadlike filaments are present on the fracture surfaces of the specimen tested at 863 K. At the same time, the local melted surfaces, which have the smooth, roundish characteristics, can be found under the long filaments. There should be no roundish fracture surface if the material was deformed under the solidus temperature of the material and the deformation completely occurs in the solid state. This is experimental evidence for the occurrence of ductile fracture, sliding of the viscous layer, and partial melting at grain boundaries and the interface between the matrix and the reinforcement, during the superplastic deformation of the composite at temperatures slightly higher than its solidus temperature.

3.4 Mechanism of High Strain Rate Superplasticity

It has been suggested[6,9,12-15] that the superplastic deformation of Al matrix composites at high strain rates is primarily due to the formation of a liquid phase at the interfaces at temperatures above, or slightly below, their incipient melting

temperatures. The presence of a liquid phase at the interfaces increases interfacial sliding between the matrix and the reinforcement and grain boundary sliding among grains at high deformation temperatures.

The incipient melting of Al matrix composites is often initiated by eutectic phases with low melting temperature at the interface between the matrix and the reinforcement, which result from chemical reaction of the segregated elements on the reinforcement surface.[9] Figure 10 shows the line distribution of Al and Si along the interface between the matrix and the reinforcement as determined by EPMA. A very high amount of silicon (Si) is present on the surface of the reinforcement particulate. A relatively low amount of Al, in comparison to that of the matrix, was also found on the surface. However, magnesium (Mg) was not detected at the interface. This may result from a reduction in Mg content in the matrix due to its oxidation during composite preparation and subsequent pretreatment processes. Examination of the Al-Si phase diagram[19] reveals that the eutectic temperature of Al-Si, 850 K, is almost the same as the incipient melting temperature of the composite (851 K). The presence of both Al and Si on the surface suggests that a eutectic reaction is possible at the interface between the matrix and the reinforcement during superplastic deformation. As a result, the superplasticity of the composite could be enhanced by the lubricating function of the liquid phase at the interface, which is produced by the eutectic reaction. However, the superplastic deformation mechanism of liquid phase may still not be sufficient to explain why the composite is capable of achieving a total elongation to failure of 438% at a temperature of 863 K and at an initial strain rate of 1.67×10^{-1} s^{-1}. Additional factors, such as dislocation associative movement and recrystallization of the matrix, may also perhaps play an important role in the superplastic deformation of the composite.

TEM analysis of the composite prior to deformation shows that a large amount of dislocations are not only present inside the grains, but are also concentrated near grain boundaries and at the interface between the matrix and reinforcement (Fig. 11). However, internal cavities and cracks along the interfaces between the matrix and reinforcement particles were not found. The high dislocation density implies that the stress concentration at grain boundary triple-point and/or near the interfaces between the matrix and the reinforcement could be released, at least in part, by an associative effect of these dislocations in a short period of time, which enables the composite to exhibit the high total elongation to failure at high strain rates during superplastic deformation. Recrystallization is often another important feature, which influences high-strain-rate superplasticity of Al metal matrix composites.[3] There should be more fine grains in the composite if the recrystallization occurs during the pretreatment or the superplastic deformation. Figure 12 shows the presence of a number of fine recrystallized grains (less than 0.5 μm) with a hexagonal shape in the matrix of the deformed composite. These grains are formed by a dynamic recrystallization process during the hot rolling pretreatment. Since one of the main deformation mechanisms for superplasticity is grain boundary sliding, the occurrence of the fine grains, which offer a large number of additional sliding interfaces, improves superplastic deformation of the composite. In addition, the hexagonal shape of the grain formed in the composite is optimum for the sliding of grain boundaries.

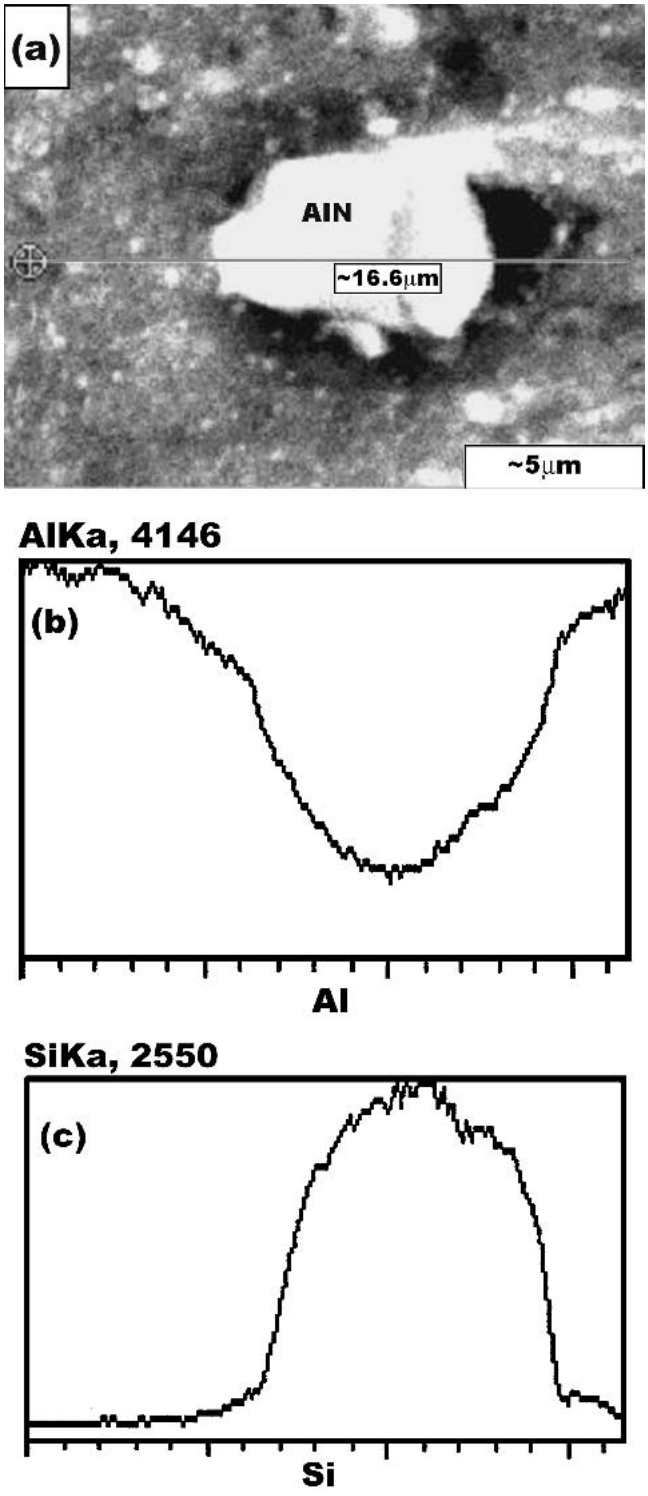

Fig. 10 Elemental line distribution of Al and Si at the surface of the reinforcement particulate (AlN)

3.5 Determination of Activation Energy

Due to the nature of superplasticity, which is a thermally activated process, the activation energy is often used as an indicator for assessing the involvement of the deformation.

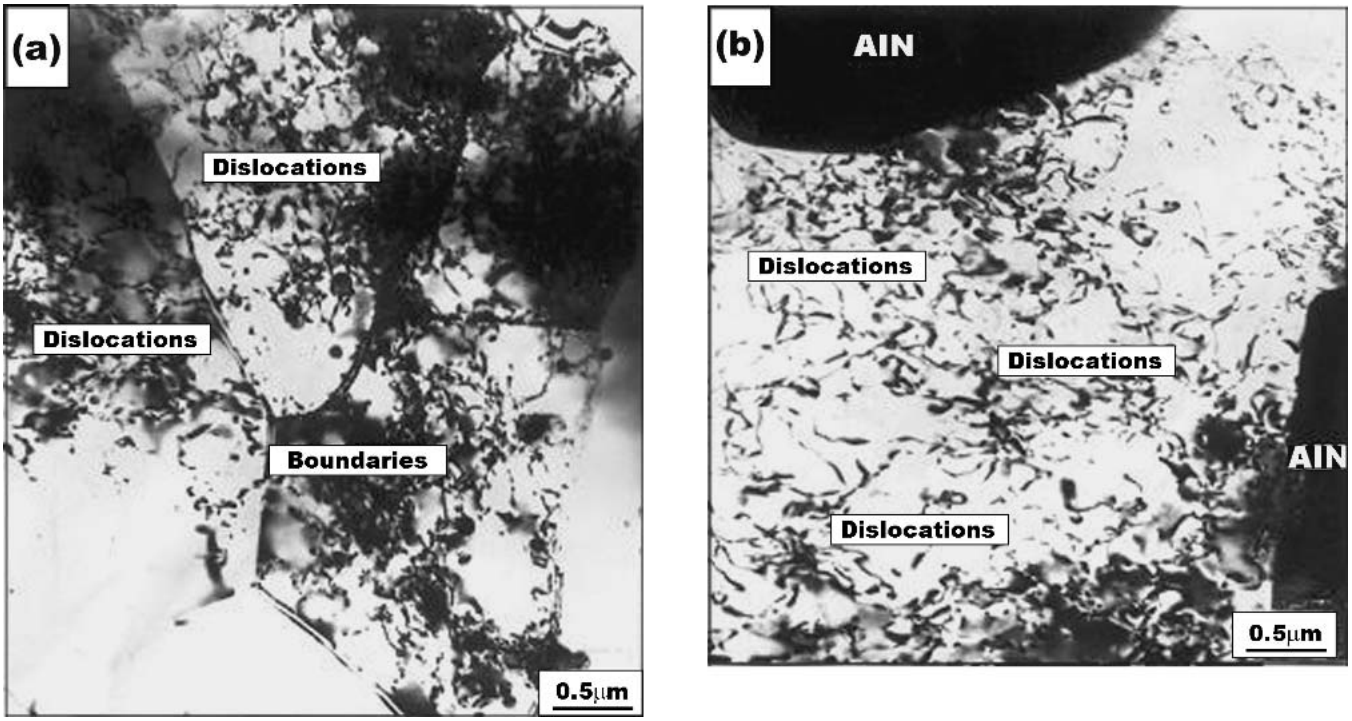

Fig. 11 TEM image of 30%AlNp/6061Al composite before superplastic deformation

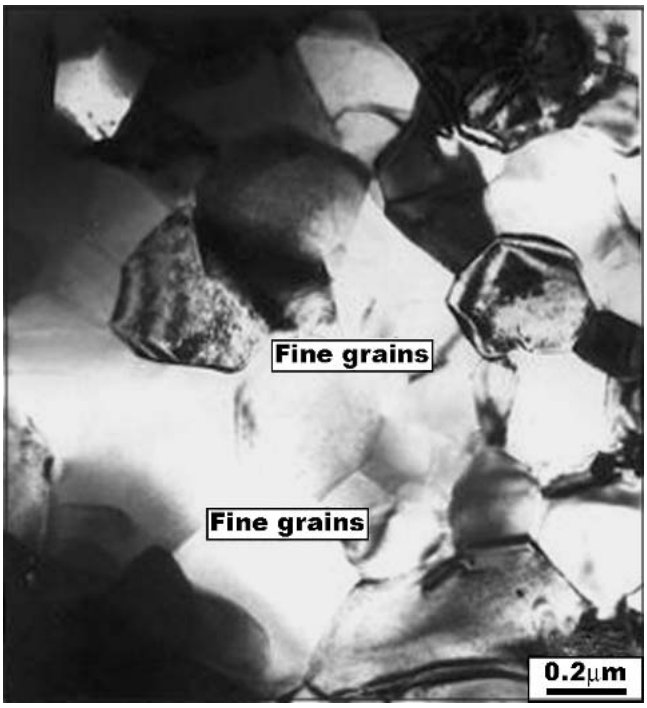

Fig. 12 TEM image of recrystallization of 30%AlNp/6061Al composite

Usually, the following power law equation[16] has been used to describe the strain rate and flow stress:

$$\dot{\varepsilon} = \frac{AGb}{kT}\left(\frac{b}{d}\right)^{p}\left(\frac{\sigma - \sigma_0}{G}\right)^{n} D_0 \exp\left(-\frac{Q}{RT}\right) \quad \text{(Eq 2)}$$

where $\dot{\varepsilon}$ is the strain rate, D_0 the diffusivity, G the shear modulus, b the Burgers vector, k the Boltzmann constant, T the test temperature, d the grain size, p the grain size exponent, σ the applied stress, σ_0 the threshold stress, $n(= 1/m)$ the stress exponent, and A is a constant. The shear modulus, G, is equal to $E/2(1 + \nu)$, where the Poisson's ratio ν is assumed to be 0.34. Assuming that the shear modulus of the composite exhibits the same dependence on temperature as that of Al,[17] the relationship between the shear modulus and the temperature for the composite can be expressed as

$$G = 4.2535 \times 10^4 - 14\,T\,(\text{MPa}) \quad \text{(Eq 3)}$$

To determine the activation energy for superplastic deformation of the composite, the following relationship at constant strain rate was derived from Eq 1

$$Q = R\,\frac{\partial \ln[(\sigma - \sigma_0)^n / G^{n-1}T]}{\partial(1/T)} \quad \text{(Eq 4)}$$

Equation 4 was used to determine the activation energy of the present composite, and its value can be compared with some theoretical values of activation energy for specific deformation mechanisms. Figure 13 is a plot of $R\ \ln[(\sigma - \sigma_0)^n / G^{n-1}T)]$ versus $1/T$ at a strain rate of 10^{-1} s^{-1} with $n = 2$. The slope of the line in Fig. 13 represents the activation energy for superplastic deformation, which is determined to be 330 kJmol^{-1} for the composite with an average reinforcement size of 1.78 μm. This value of the activation energy is higher than the activation energy for lattice self-diffusion in Al alloys (142 kJ mol^{-1}).[17] However, it is very similar to the values of the

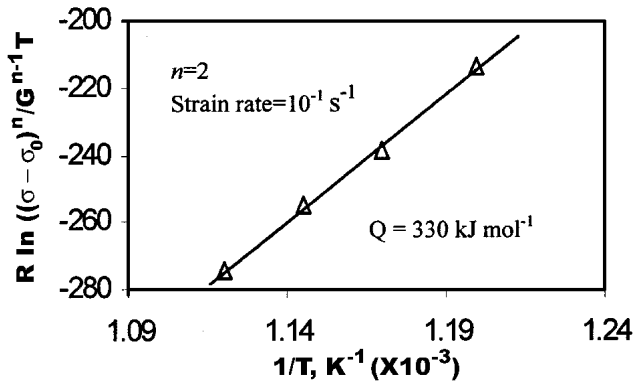

Fig. 13 Plot of $R \ln [(\sigma - \sigma_0)^n/G^{n-1}T)]$ versus $1/T$ at a strain rate of 10^{-1} s^{-1} with $n = 2$

activation energies for other superplastic Al-MMCs[17] [282 $kJmol^{-1}$ for Si_3N_4p(0.1 μm)/Al-Mg-Si composite, 327 $kJmol^{-1}$ for Si_3N_4p(0.2 μm)/Al-Mg composite and 567 $kJmol^{-1}$ for Si_3N_4w/Al-Cu-Mg composite].

4. Conclusions

It is shown that a 30 vol.% AlNp/6061Al composite prepared by a PM method and hot-rolled after extrusion exhibits a maximum superplastic elongation of 438% at a temperature of 863 K at an initial strain rate of 1.67×10^{-1} s^{-1}. The long filament microstructural features on the fracture surfaces of the composite superplastically deformed at the optimum test temperature indicate the presence of grain boundary sliding and phase melting at the interface. The occurrence of a liquid phase at the interface by partial melting at elevated temperature may result from the concentration of Si at the interface. Dislocations at the interfaces and inside the grains play a very important role in reducing the stress concentration at grain boundary triple-points or at the interface between the matrix and the reinforcement. The recrystallization process contributes to the refinement of grain size. These combined effects maximize the total elongation to failure of the composite at high strain rates.

Acknowledgments

This work was supported by the National Natural Scientific Foundation of China, under Project No. 59781004, and by the Open Project Foundation of State Key Laboratory of Rolling and Automation, Northeastern University, China. Also, the authors would like to take this opportunity to thank the Natural Sciences and Engineering Research Council of Canada for the Provision of Discovery Grants to Dr. Northwood and Dr. Hu in support of this work.

References

1. T.G. Nieh, C.A. Henshall, and J. Wadsworth: "Superplasticity at High-Strain Rates in A SiC Whisker Reinforced Al-alloy," *Scripta Metall.,* 1984, *18,* pp. 1405-08.
2. T. Hikosaka and T. Imai: "Effect of Hot Rolling on Superplasticity of A SiC/6061 Aluminum Alloy Composite Made By A Vortex Method," *Scripta Mater.,* 1997, *36*(2), pp. 145-50.
3. W.J. Kim: "The Effect of Reinforcement on Superplastic Flow in Powder-Metallurgy Processed Aluminum Matrix Composites," *Key Eng. Mater.,* 2000, *177-180*(2), pp. 643-48.
4. G.Q. Tong and K.C. Chan: "Deformation Behavior of A PM Al6013/SiCp Composite Sheet at Elevated Temperature," *Mater. Lett.,* 1999, *38*(5), pp. 326-30.
5. L.H. Han, J.T. Niu, and D.M. Jiang: "Superplasticity in An Aluminum Alloy 6061/AlOComposite," *J. Mater. Sci. Technol.,* 2001, *17*(6), pp. 653-56.
6. M. Mabuchi, K. Higashi, K. Inoue, and S. Tanimura: "Experimental Investigation of Superplastic Behavior in A 20 Vol. Percent Si_3N_4p/5052-Aluminum Composite," *Scripta Metall. Mater.,* 1992, *26,* pp. 1839-44.
7. M. Mabuchi, K. Higashi, Y. Okada, S. Tanimura, T. Imai, and K. Kubo: "Very High Strain-Rate Superplasticity in A Particulate Si_3N_4/6061 Aluminum Composite," *Scripta Metall. Mater.,* 1991, *25,* pp. 2517-22.
8. B.Q. Han and K.C. Chan: "High-strain-rate Suuperplasticity of An Al6061-SiCw Composite," *Scripta Mater.,* 1997, *36,* pp. 593-98.
9. M. Mabuchi, K. Higashi, and T.G. Langdon: "An Investigation of The Role of A Liquid-phase in Al-Cu-Mg Metal-Matrix Composites Exhibiting High-Strain Rate Superplasticity," *Acta Metall. Mater.,* 1994, *42,* pp. 1739-45.
10. T. Imai, G.L'Esperance, and B.D. Hong: "High-Strain Rate Superplasticity of AlN Particulate-reinforcement Aluminum-alloy Composites," *Scripta Metall. Mater.,* 1994, *31,* pp. 321-26.
11. M. Mabuchi and K. Higashi: "High-Strain-Rate Superplasticity in Magnesium Matrix Composites Containing Mg_2Si Particles," *Philos. Mag. A,* 1996, *74,* pp. 887-905.
12. G. Nieh and J. Wadsworth: "High-Strain-Rate Superplasticity in Aluminum Matrix Composites," *Mater. Sci. Eng. A,* 1991, *147,* pp. 129-42.
13. T. Imai, S. Kojima, G. L'Esperance, B. Hong, and D. Jiang: "Effect of Volume Fraction of AlN Particle on Superplasticity of AlN/6061 Aluminum Alloy Composite," *Scripta Mater.,* 1996, *35,* pp. 1199-1204.
14. O.A. Kaibyshev, V. Kazyhanov, and C.C. Bampton: "Superplastic Deformation of the 2009-15%SiCw Composite," *Key. Eng. Mater.,* 1997, *127-131,* pp. 953-60.
15. K. Matsuki, M. Tokizawa, and S. Murakami: "Effect of SiC Particulate Content on Superplastic Flow Stress of MA 2024Al-SiCp Composites," *Mater. Sci. Form,* 1997, *243-245,* pp. 309-14.
16. R.S. Mishra, T.R. Bieler, and A.K. Mukherjee: "Mechanism of High Strain Rate Superplasticity in Aluminum Alloy Composites," *Acta Mater.,* 1997, *45,* pp. 561-68.
17. M. Mabuchi and K. Higashi: "Activation Energy for Superplastic Flow in Aluminum Matrix Composites Exhibiting High-Strain–Rate Superplasticity," *Scripta Metall.,* 1996, *34,* pp. 1893-97.
18. G.E. Dieter, *Mechanical Metallurgy,* McGraw-Hill, New York, 1986, pp. 295-301.
19. T. B. Massalski, *Binary Alloy Phase Diagrams,* American Society for Metals, Metals Park, OH, 1986.